# Vessel discoloration detection in malarial retinopathy

C. Agurto[a], S. Nemeth[a], S. Barriga[a], P. Soliz[a], I. MacCormick[b], T. Taylor[c], S. Harding[b], S. Lewallen[d], V. Joshi[a]

[a]VisionQuest Biomedical LLC, Albuquerque, NM, USA; [b]University of Liverpool, Liverpool, UK; [c]Michigan State University, East Lansing, MI, USA; [d]Kilimanjaro Centre for Community Ophthalmology, Cape Town, South Africa.

## ABSTRACT

*Cerebral malaria (CM) is a life-threatening clinical syndrome associated with malarial infection. It affects approximately 200 million people, mostly sub-Saharan African children under five years of age. Malarial retinopathy (MR) is a condition in which lesions such as whitening and vessel discoloration that are highly specific to CM appear in the retina. Other unrelated diseases can present with symptoms similar to CM, therefore the exact nature of the clinical symptoms must be ascertained in order to avoid misdiagnosis, which can lead to inappropriate treatment and, potentially, death. In this paper we outline the first system to detect the presence of discolored vessels associated with MR as a means to improve the CM diagnosis. We modified and improved our previous vessel segmentation algorithm by incorporating the 'a' channel of the CIELab color space and noise reduction. We then divided the segmented vasculature into vessel segments and extracted features at the wall and in the centerline of the segment. Finally, we used a regression classifier to sort the segments into discolored and not-discolored vessel classes. By counting the abnormal vessel segments in each image, we were able to divide the analyzed images into two groups: normal and presence of vessel discoloration due to MR. We achieved an accuracy of 85% with sensitivity of 94% and specificity of 67%. In clinical practice, this algorithm would be combined with other MR retinal pathology detection algorithms. Therefore, a high specificity can be achieved. By choosing a different operating point in the ROC curve, our system achieved sensitivity of 67% with specificity of 100%.*

**Keywords:** malarial retinopathy, vessel discoloration, vessel segmentation.

## 1. INTRODUCTION

A potentially fatal consequence of malarial infection is cerebral malaria (CM). In 2013, 198 million people worldwide were infected with malaria, which led to over half a million deaths. 75% of these fatalities were African children under five years of age [1]. Autopsies showed that 23% of the children were misdiagnosed with CM, [2] demonstrating the need for alternative methods for CM diagnosis. A study [3] has found that specific retinal lesions known as malarial retinopathy (MR) are associated with CM. Pathologies such as retinal whitening, white-centered hemorrhages and vessel discoloration are unique to MR. These features are partially related to ischemia, and are associated with processes occurring in the brain that lead to coma in malaria patients [4].

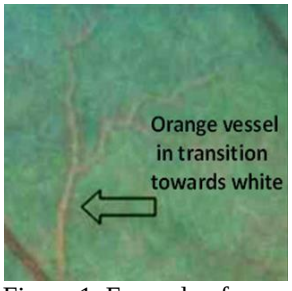

Figure 1. Example of vessel discoloration.

This paper presents a method for detecting discolored vessels in subjects with MR. The main characteristic of this pathology is the discoloration of retinal vessels from red to orange or to white. The discoloration can occur in sections of vessel, continuous or interrupted [5]. In [6], the authors proposed that discoloration is caused by the de-hemoglobinization of parasitized erythrocytes. Vessel discoloration affects capillaries, venules, and arterioles. Since vessel discoloration is more prominent in the periphery, a specific ophthalmoscopy technique is used [5].

Very few studies have addressed automatic detection of MR pathologies such as hemorrhages [7,8], whitening [9], and vessel abnormalities [10]. To the best of our knowledge, there is no previous work on detecting vessel discoloration due to MR in retinal fundus images.

In Section 2 of this paper, the dataset is described, as well as the methods used in the study. In Section 3, results are shown. Discussion and conclusions are presented in Section 4.

## 2. DATASET AND METHODS

### 2.1 Dataset

The University of Liverpool provided retrospective cases that were acquired in a malaria ward in Malawi, Africa between the years 2006 and 2014. The dataset consists of 40 mosaic images generated by stitching several images acquired with a Topcon 50EX retinal camera having a field of view (FOV) of 50˚. The distribution of cases was 31 with discoloration and 9 with normal vasculature.

A reference standard to train our algorithms was provided by a certified ophthalmic medical technologist (COMT) who annotated the discolored vessels in the mosaic images.

### 2.2 Methods

Fig 2 shows the block diagram of the proposed system to detect discolored vessels. First, we perform vasculature segmentation by combining information from different color channels. Then, we divide the vasculature into vessel segments and extract color features from each of them. Finally, we apply a partial least square classifier to determine which vessel segments present discoloration. Each element of the system is described in the following sections.

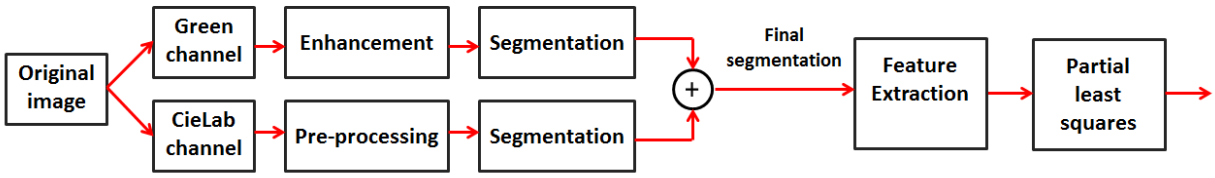


Figure 2. Block diagram of the system to detect vessel discoloration

#### a) Vessel segmentation

To detect discoloration, we first segment the vessels in the image. To accomplish this task, we combine the segmentation of two color channels (green and 'a' from CIELab color space), as indicated in Fig 2.

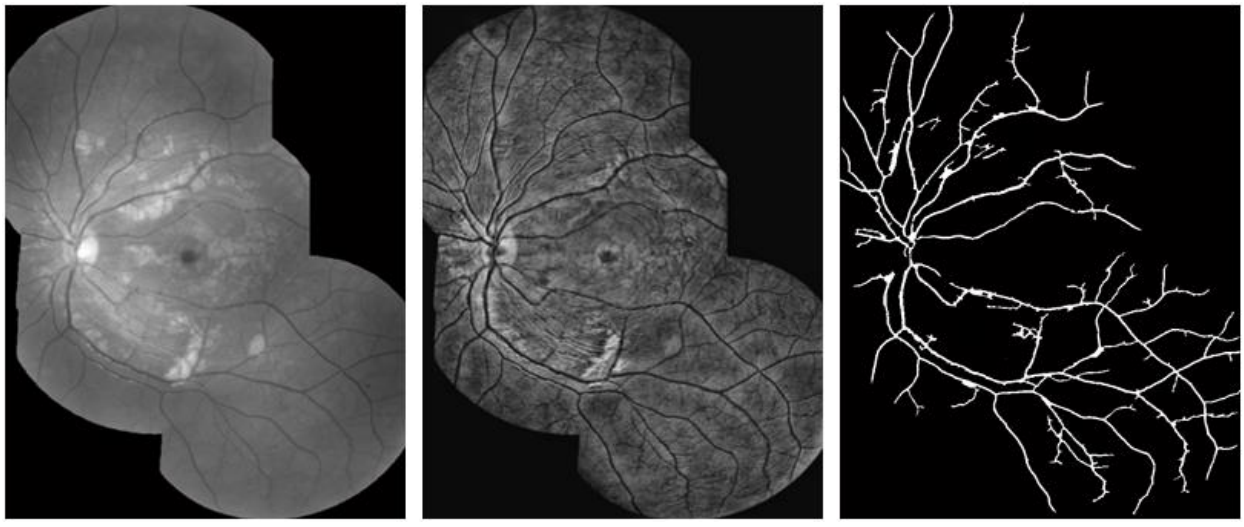

(a) (b) (c)

Figure 3. Results of segmentation in the green channel. a) Original image; b) enhanced image with CLAHE; c) vessel segmentation results.

First, we increased the contrast of the green channel of the image in Fig. 3a using contrast limited adaptive histogram equalization (CLAHE) [11] with a matching exponential distribution (Fig. 3b). Then, we enhanced the vessels using multiscale Frangi filters [12]. We set sigma values in the range of [3 7] for the Gaussian kernels of the Frangi filters. After obtaining the vessel enhancement map, we improved the segmentation described in [13] by increasing contrast in the map and by performing morphological operations on the binary map obtained after entropy thresholding [14] to remove the noise iteratively. Fig. 3c shows the results of segmentation in the green channel. However, not all of the vessels were captured in this channel, especially some of the thin discolored ones. We improved the segmentation by incorporating information from the 'a' channel of the CIELab color space. This color space captures information from some of the vessels that are small and discolored, and that the green channel failed to capture. Therefore, we segmented the information from this color space to complement the segmentation found with the green channel. After removing the segmented vessels, we inverted the color and increased the contrast of the image using CLAHE with uniform distribution matching (Fig 4b).

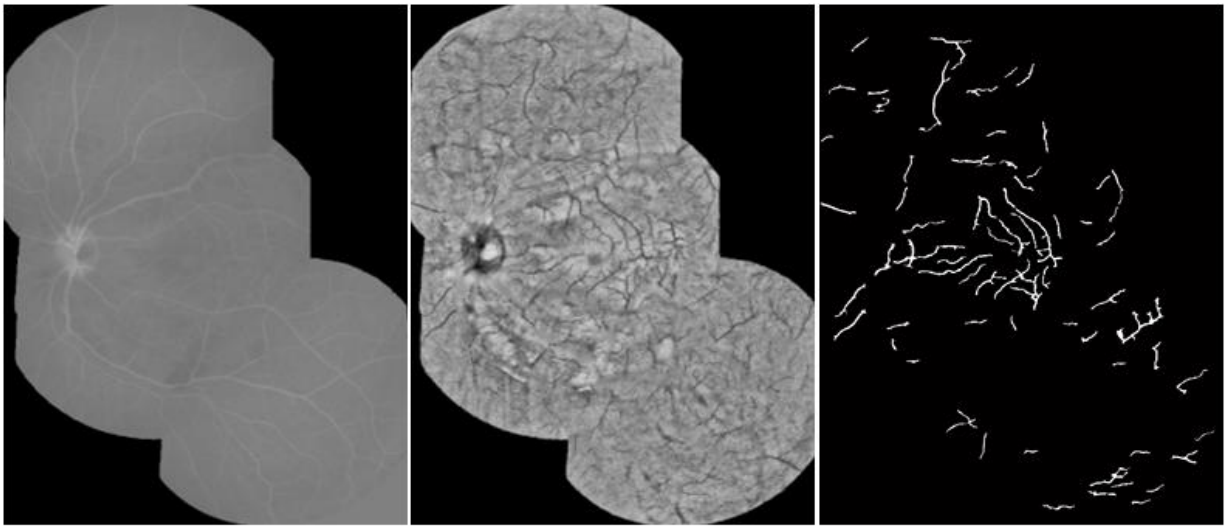

(a) (b) (c)

Figure 4. Results of segmentation using the 'a' channel of the CIELab. a) 'a' channel of CIELab; b) enhanced image after removing the vessels in (a); c) segmentation results of (b).

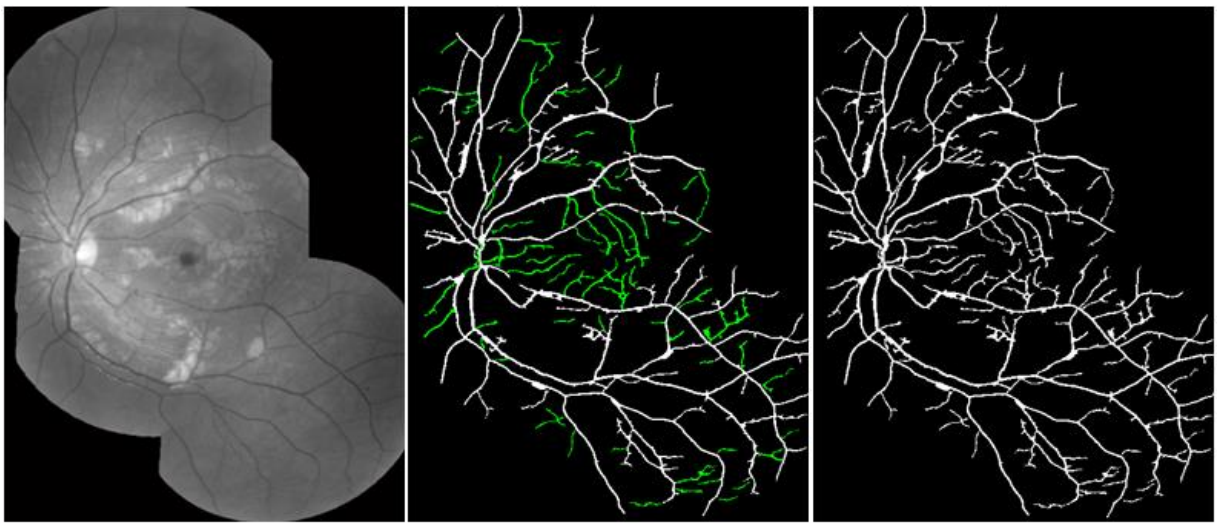

(a) (b) (c)

Figure 5. Final segmentation results for images with vessel discoloration. a) Original image; b) segmentation results of Fig. 3 in white and Fig. 4 in green; c) final segmentation.

Finally, we segmented the vessel by applying the same approach used for the green channel, but changing the size of the Frangi filters to have sigma values in the range of [1 5], since these vessels are narrower than the ones in the green channel. Finally, we added both segmentation results to obtain our final segmentation, as shown in Fig. 5c.

### b) Feature extraction

Before feature extraction, the segmented vasculature is partitioned into vessel segments. We first skeletonized the segmented vasculature. Then, we found the branches and crossing points using morphological operations, and removed them from the skeletonized vasculature. The remaining lines are the vessel segments to be analyzed.

To extract features for each vessel segment, we took into consideration three important aspects of the discolored vessels: (a) the discolored vessels range from orange to white; (b) the edge of the vessel wall has low contrast; and (c) the regions close to the wall become discolored at the outset, when the pathology appears. Taking into account these factors, we extracted features using color information from the various color spaces (RGB, YIQ, YCbCr, CIELab, HSV) in the center of the vessel and in the vessel wall. In addition, we calculated the gradient of red, green, and 'a' channels to measure the contrast of the vessel close to the boundary.

Because we used color features, a normalization step is required. However, color normalization can generate artifacts. To avoid this, instead of obtaining absolute values for the features, we computed features using relative values. Keeping in mind the fact that wide vessels located close to the optic disc do not present discoloration, we created a "normal vasculature binary map" by enhancing the vessels in the green channel and thresholding them using $10^{th}$ percentile information. We used this binary map as a reference for normal vessels when we calculated the features. For each channel space, we computed the mean of the intensity of the area occupied for the normal vasculature map and subtracted this reference quantity for each pixel in the color space. This resulted in the distance of the pixel with respect to the mean of the normal vasculature as the feature used in the classification stage.

To summarize, we extracted features from 15 color channels and three gradient images. Since we wanted to classify vessel segments and our information is in pixels, we computed the values of the $50^{th}$, $75^{th}$, and $95^{th}$ percentiles for all the content in the analyzed vessel segment. Our feature space consisted of 108 features, 54 each for the vessel wall and vessel center.

### c) Classification

In order to reduce the amount of information, we defined two rules for classification: (a) A valid segment has at least 100 pixels of centerline (approximately one third the diameter of the optic disc; and (b) an abnormal segment is determine by a 50% overlapping between the segmented vessel and reference standard marked by a retinal specialist. By using the information from the classes, we applied a linear regression classifier known as partial least squares [15]. The classification results were validated using 5-fold cross validation.

## 3. RESULTS

A total of 4598 vessel segments were extracted from the vasculature of the 40 cases. The vessel segments were processed with our methodology, obtaining the ROC curve shown in Figure 6a. The AUC for vessel segmentation was 0.90 with best sensitivity/specificity of 90%/70%. A maximum accuracy of 89% was achieved.

Since the main purpose of this approach is MR diagnosis, we calculated the performance of the classification per image. We counted the number of segments in the images that were classified as discolored. To determine which vessel segments are considered discolored, we fix a point in the ROC curve (Fig. 6a), which represents a sensitivity/specificity of 82%/83% of the vessel segment classification. Then, we used the number of abnormal segments in the image to perform the image classification. The more segments we find, the more the image is likely to have MR. We obtained an AUC of 0.87 for image classification with maximum accuracy of 85% and best sensitivity/specificity of 94%/67% as one pathology detection algorithm. Higher specificity of 100% with sensitivity of 68% can be obtained by choosing a different operating point in the ROC curve for image classification shown in Fig. 6b. High specificity is required because the main goal is to develop a MR detection system, so that algorithms developed for the detection of other MR pathologies (such as hemorrhages or whitening) will be combined. An example of our detection system is shown in Figure 7, where the detected discolored vessels are marked in blue.

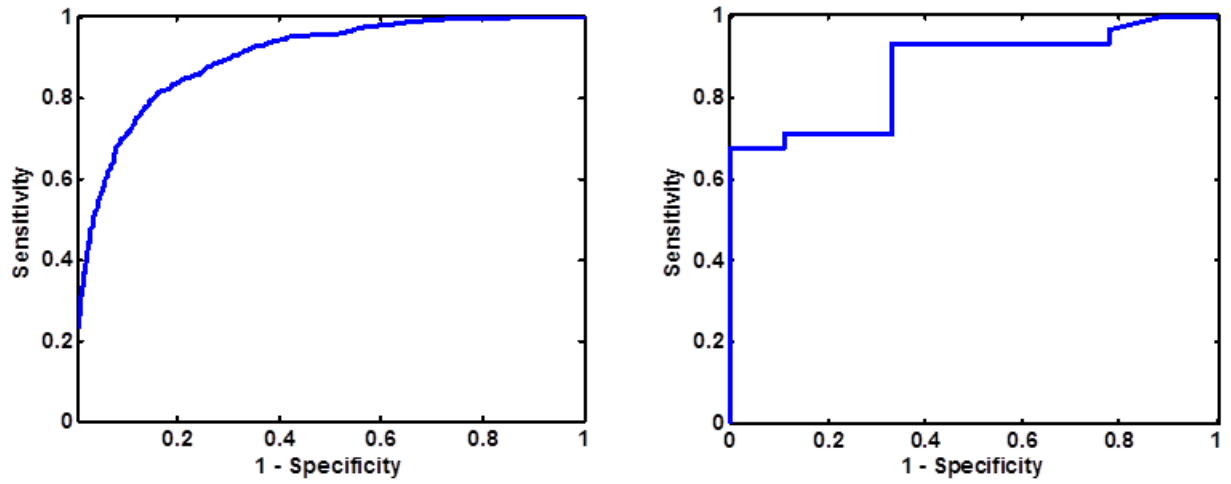


(a) (b)

Figure 6. (a) ROC curve for vessel segment classification; (b) image classification.

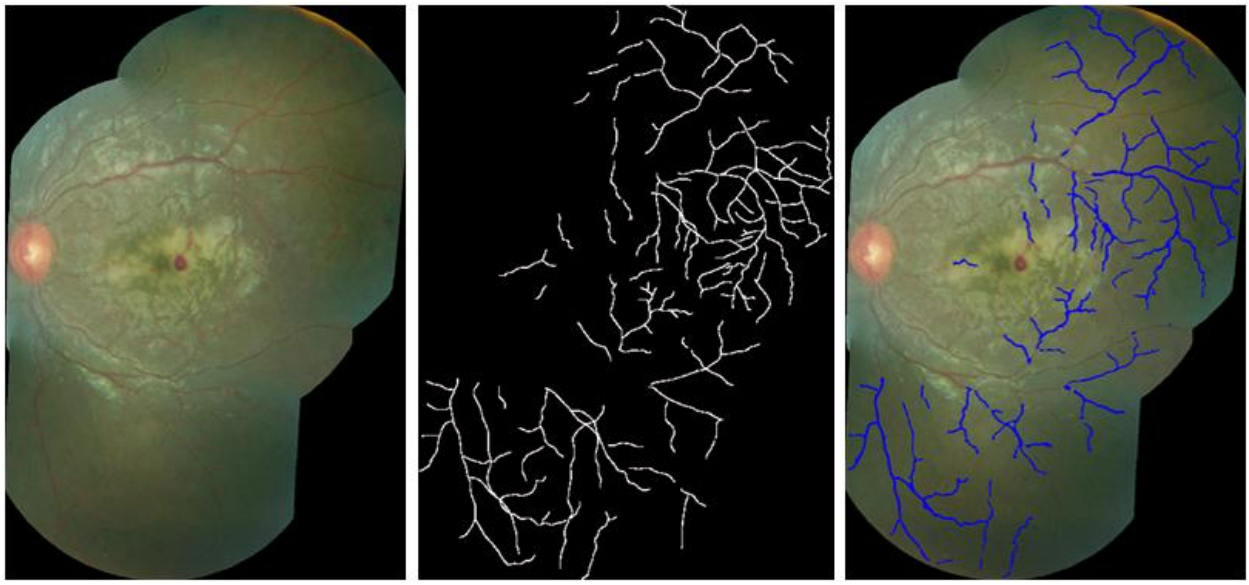

(a) (b) (c)

Figure 7. Results of image classification. a) Original image; b) reference standard; c) automated discoloration detection marked in blue.

## 4. DISCUSSION AND CONCLUSIONS

We have developed the first automatic algorithm for the detection of discolored vessels due to malarial retinopathy in retinal images. Our implementation consists of an improved vessel segmentation algorithm that can segment vessels with discoloration, along with robust feature extraction that helps us achieve high detection rates for vessel segment and image classification. The system provides high accuracy detection of 85% with sensitivity/specificity of 68%/100%.

Vascular segmentation algorithms applied to retinal images use the green channel as a basis for their segmentation. However, discolored vessels do not present high contrast with respect to the retinal background, as do normal vessels. Therefore, it is important to use other color spaces to complement the information.

Another common problem in detection algorithms that rely primarily on color information in the feature set (such as the one presented here) is inter-patient variability caused by various factors, for example the race of the analyzed subjects. For that reason, we present a method that uses relative measurements instead of absolute values. In so doing, we provide a more robust classification process, with high detection rates.

For the classification of images, we used as feature the number of detected abnormal segments. Other methods may also be explored, such as the mean estimated class among detected segments. In this case, the former method was used because most of the abnormal cases present many discolored vessels.

Finally, vessel discoloration is seen primarily at the periphery of the retina, therefore the use of a single standard image (~ FOV of 45˚) for the detection of this pathology is not recommended. A higher degree of FOV camera, or stitching different field images to create a mosaic image (as we used in the present study), is necessary for correct detection.

**Acknowledgements**

This work was funded by the National Institute of Allergy and Infectious Diseases grant no. 2R44AI112164-03.

## References

[1] World Health Organization Global Malaria Program, *World Malaria Report*, December 2013.

[2] Taylor, T. E., Fu, W. J., Carr, R. A., Whitten, R. O., Lewallen, S., Liomba, N. G., Molyneux, M. E., "Differentiating the pathologies of cerebral malaria by postmortem parasite counts," *Nat Med.* **10**, 143-145 (2004).

[3] Lewallen, S., Taylor, T.E., Molyneux, M. E., Wills, B. A., Courtright, P., "Ocular fundus findings in Malawian children with cerebral malaria," Ophthalmology **100**, 857-861 (1993).

[4] White, V., Lewallen, S., Beare, N., "Retinal pathology of pediatric cerebral malaria in malawi," *PLoS One* **4**(1), e4317 (2009).

[5] Beare, N. A. V., Taylor, T. E., Harding, S. P., Lewallen, S., Molyneux, M. E., "Malarial retinopathy: a newly established diagnostic sign in severe malaria," *Am J Trop Med Hyg* **75**, 790-797 (2006).

[6] Lewallen, S., White, V. A., Whitten, R. O., Gardiner, J., Hoar, B., Lindley, J., et al., "Clinical-histopathological correlation of the abnormal retinal vessels in cerebral malaria," *Arch Ophthalmol* **118**, 924–928 (2000).

[7] Saleem, M., Usman, A. M, "Detection of hemorrhages for diagnosis of malarial retinopathy," *Biomedical Engineering Conference (CIBEC)*, 141-144 ( 2014)

[8] Joshi, V.S., Maude, R. J., Reinhardt, J. M., Tang, L., Garvin, M. K., Sayeed, A., Ghose, A., Hassan, M. U., Abràmoff, M.D., "Automated detection of malarial retinopathy-associated retinal hemorrhages," *Invest Ophthalmol Vis Sci.* ***53(1)***, 6582-6588 (2012)

[9] Zhao, Y., MacCormick, I., Parry, D. G., Leach, S., Beare, N. A. V., Harding, S. P., Zheng, Y., "Automated Detection of Leakage in Fluorescein Angiography Images with Application to Malarial Retinopathy," *Scientific Reports 5*, 10425 (2015).

[10] Zhao, Y., MacCormick, I., Parry, D. G., Beare, N. A. V., Harding, S. P., Zheng, Y., "Automated Detection of Vessel Abnormalities on Fluorescein Angiogram in Malarial Retinopathy," *Sci. Rep.* **5**, 11154 (2015).

[11] Zuiderveld, K., "Contrast Limited Adaptive Histograph Equalization," *Graphic Gems IV. San Diego: Academic Press Professional*, 474–485 (1994).

[12] Frangi, A. F., Niessen, W. J., Vincken, K. L., and Viergever, M. A., "Multiscale Vessel Enhancement Filtering". *In Wells, WM, Colchester, A, & Delp, S, Editors, MICCAI '98 Medical Image Computing and Computer-Assisted Intervention, Lecture Notes in Computer Science, Springer Verlag*, 130-137 (1998).

[13] Yu, H., Barriga, S., Agurto, C., Zamora, G., Bauman, W., Soliz, P., "Fast Vessel Segmentation in Retinal Images Using Multiscale Enhancement and Second-order Local Entropy, " *Proc. SPIE* **8315**, 83151B (2012)

[14] Chanwimaluang, T., Guoliang, F., "An efficient blood vessel detection algorithm for retinal images using local entropy thresholding," in Circuits and Systems, *ISCAS '03*, V-21-V-24 (2003)

[15] de Jong, S., ''SIMPLS: An alternative approach to partial least squares regression,*'' Chemometrics and Intelligent Laboratory Systems* **18**, 251-263 (1993).